Reprinted from Journal of the Optical Society of America B, Vol. 2, page 1721, November 1985
Copyright © 1985 by the Optical Society of America and reprinted by permission of the copyright owner.

Angular momentum of trapped atomic particles

D. J. Wineland, J. J. Bollinger, Wayne M. Itano, and J. D. Prestage

Time and Frequency Division, National Bureau of Standards, Boulder, Colorado 80303

Received April 10, 1985; accepted July 23, 1985

In axially symmetric atomic-particle traps, the angular momentum of the particles about the symmetry axis is conserved in the absence of external torques. Changes in this angular momentum owing to laser scattering are discussed.

1. INTRODUCTION

By now, one has become fairly familiar with the idea that the momentum carried by light can be transferred to atomic (or macroscopic) particles, thereby significantly altering the velocity distribution of these particles. The status of experiment and theory will be discussed in the accompanying papers of this issue; further information can be found in other recent papers.[1–3]

In the experiments on atomic deflection and laser cooling, one is concerned primarily with the changes in linear mechanical momentum imparted to the particles by light. However, for the case of trapped particles, one must in general be concerned with the angular momentum of the trapped particles and therefore with the changes in angular momentum of the trapped particles by light. The situation discussed in this paper is illustrated in Fig. 1. If the trap (trapping fields are not shown) is symmetric about a particular axis, here assumed to be the z axis, then one would expect the z component of angular momentum of the particles, L_z, to be conserved in the absence of laser scattering. Here, L_z is the total canonical angular momentum given by

$$L_z = \sum_{i=1}^{N} l_{zi} = \sum_{i=1}^{N} (\mathbf{x}_i \times \mathbf{p}_i)_z, \tag{1a}$$

$$\mathbf{p}_i = m_i\mathbf{v}_i + q_i\mathbf{A}(\mathbf{x}_i)/c, \tag{1b}$$

where l_{zi}, $\mathbf{p}_i$, m_i, q_i, $\mathbf{x}_i$, and $\mathbf{v}_i$ are the z component of angular momentum, the linear momentum, mass, charge, position, and velocity of the ith particle, respectively; N is the number of particles; c is the speed of light; and $\mathbf{A}$ is the vector potential. From the geometry of Fig. 1, it is clear that the laser scattering can be used to increase $|L_z|$ indefinitely, *independently of the laser tuning*. This effect would be interesting to study, but of course in experiments employing laser cooling it is clearly a situation to be avoided. In practice, changes in angular momentum will also be influenced by various mechanisms, such as collisions with background gas and deviations of the trap from axial symmetry.

Assuming that the laser beam is perpendicular to $\hat{z}$, the magnitude of the average change of mechanical angular momentum per photon-scattering event is given by hd/λ, where d is the distance of the laser beam from the z axis, h is Planck's constant, and λ is the wavelength of the photons. Changes in the internal angular momentum of atomic particles will be of order $\hbar$. Typically, $2\pi d/\lambda \gg 1$; therefore we will neglect the internal angular momentum of the particles. As in previous treatments,[4,5] for simplicity we will neglect second-order relativistic effects and saturation. We will also assume that the collision rate between trapped particles is high enough and the laser scattering rate low enough that the particles can be assumed to be in thermal equilibrium. These conditions may be violated, but the qualitative features of the problem should still apply.

To make the problem more tractable, we will discuss only angular-momentum effects in ion traps, specifically, the rf (Paul) and Penning traps.[6–11] This seems reasonable, since many experiments have been done with these traps. The qualitative features of these traps should carry over to neutral traps. The primary difference would seem to arise from the absence of long-range Coulomb repulsion between particles and the fact that the field momentum that is due to the ions' net charge [vector-potential term in Eq. (1)] is absent. Finally, in this paper angular-momentum changes are assumed to arise from laser scattering, background gas, and trap asymmetries; however, such effects may come from scattering by particle beams,[12] positive or negative feedback on the charged-particle motions,[12,13] or angular-momentum transfer from plasma waves.[14,15]

In Section 2, we will assume that ion trapping is accomplished by a combination of rf and Penning traps. For such a combined trap, single-particle trajectories have been discussed by others[9–11]; here we will use the pseudopotential approach.[6,7,9–11] Assuming that the ion cloud (or nonneutral plasma[13–15]) rotates at a frequency ω about a particular symmetry axis, we derive relations between ω and the ion cloud's density, potential, dimensions, and angular momentum. These expressions can then be applied to the rf or the Penning trap in various limits. In Section 3 we discuss torques applied to the cloud from laser scattering for a particular ion-cloud–laser-beam interaction geometry. Background-gas damping is discussed in Section 4. Changes in angular momentum owing to trap asymmetries are treated separately for the rf and the Penning traps in Sections 5 and 6, respectively. Finally, in Section 7, we make a few remarks about angular momentum in neutral-particle traps.

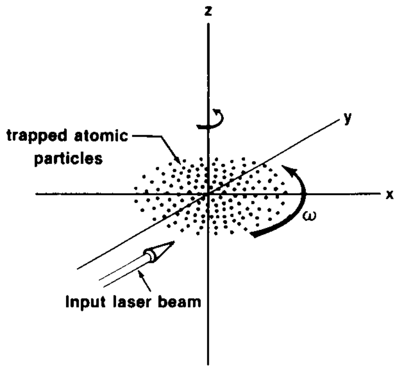

Fig. 1. Schematic representation of trapped atomic particles. The trap (not shown) is assumed to have axial symmetry about the z axis. If a laser beam is directed parallel to the y axis but does not intersect the z axis, then atomic particle–photon scattering imparts angular momentum (L_z) to the sample, which can cause it to spin about the z axis.

2. ION TRAPS

For further simplicity, we will assume idealized models for the rf and Penning traps and assume only one trapped ion species. Both traps use axially symmetric electrodes whose surfaces are figures of revolution (hyperboloids of revolution) as shown in Fig. 2. For rf trapping, when the drive (micromotion) frequency Ω is much larger than secular frequency ω_x, ω_y, or ω_z (defined in Section 5), the ions can be considered to be confined in the axially symmetric pseudopotential[6–11] of the form

$$\phi_T(r, z) = \alpha r^2 + \beta z^2, \tag{2}$$

where r and z are cylindrical coordinates and α and β are functions of the trapping parameters:

$$\alpha = qV_0^2/m\Omega^2\xi^4 - U_0/\xi^2, \tag{3a}$$

$$\beta = 4qV_0^2/m\Omega^2\xi^4 + 2U_0/\xi^2. \tag{3b}$$

V_0 is the amplitude of the rf voltage, U_0 is the amplitude of the dc voltage applied between the ring and the end caps (here, U_0 positive means that the end caps are at higher potential than the ring electrode), and $\xi^2 = r_0^2 + 2z_0^2$, where r_0 and z_0 are defined in Fig. 2. We note that the pseudopotential [the first terms in Eqs. (3a) and (3b)] always acts to give a radially inward force (independent of the sign of q) while the force that is due to the dc applied potential can be in either direction. For the rf trap we want $q\alpha$, $q\beta > 0$; the resulting potential well is equivalent to that provided by a uniform-background charge distribution whose boundary is an ellipsoid of revolution.[16] From Poisson's equation, $\nabla^2\phi = -4\pi\rho$, we see that the density inside this fictitious charge distribution is given by $\rho' = -(2\alpha + \beta)/2\pi$. The potential for the Penning trap[6,7] is usually given by Eqs. (2) and (3) with $V_0 = 0$; in this case a magnetic field $\mathbf{B} = B_0\hat{z}$ is required for trapping. For the sake of generality we will assume that $B_0 \neq 0$ and $V_0 \neq 0$ except where noted below.

The traps have symmetry about z, and, therefore, in the absence of external torques, L_z is conserved. In this case, the ion canonical angular momentum and ion energy enter the thermal-equilibrium distribution function on an equal basis. The thermal-equilibrium distribution function can be written as[17–19]

$$f = n_0\left(\frac{m}{2\pi k_B T}\right)^{3/2} \exp[-(H - \omega l_z)/k_B T], \tag{4}$$

where

$$H = mv^2/2 + q\phi(\mathbf{x}) \tag{5a}$$

is the ion energy and

$$l_z = mv_\theta r + qA_\theta(\mathbf{x})r/c \tag{5b}$$

is the ion canonical angular momentum. m, q, and $\mathbf{v}$ are the ion mass, charge, and velocity, and $v = |\mathbf{v}|$. v_θ and A_θ are the θ components of the velocity and the vector potential, and r is the radial coordinate of the ion in cylindrical coordinates. $\phi = \phi_I + \phi_T + \phi_{\text{ind}}$ is the total potential, which is written as the sum of the potential that is due to ion space charge ϕ_I, the applied trap potential ϕ_T, and the potential ϕ_{ind} that is due to the induced charges on the trap electrodes. n_0, T, and ω are determined by the total number of ions, energy, and angular momentum of the system, and k_B is Boltzmann's constant. We choose the symmetric gauge where $\mathbf{A}(\mathbf{x}) = \mathbf{B} \times \mathbf{x}/2$, so that $A_\theta = Br/2$. We can therefore write the distribution function as[19]

$$f(\mathbf{x}, \mathbf{v}) = n(\mathbf{x})\left(\frac{m}{2\pi k_B T}\right)^{3/2} \exp[-\tfrac{1}{2}m(\mathbf{v} - \omega r\hat{\theta})^2/k_B T], \tag{6a}$$

where $n(\mathbf{x})$ is the ion density given by

$$n(\mathbf{x}) = n_0 \exp\left\{-\left[q\phi(r, z) - \tfrac{1}{2}m\omega\left(\frac{q}{|q|}\Omega_c + \omega\right)r^2\right]\Big/k_B T\right\}. \tag{6b}$$

We assume that the trap potential is adjusted to make $\phi = 0$ at the origin, in which case n_0 is the ion density at the center of the trap. $\Omega_c = |qB/mc|$ is the cyclotron frequency. With the assumption that $v \ll c$, we have neglected the diamagnetic correction to the magnetic field that is due to the motion of the ions. For densities near the maximum density (discussed below) this assumption may break down for electrons.

Equations (6) have been analyzed for the case of electrons in a Penning-type geometry (axially symmetric but nonquadratic trap potential).[18,19] We can easily extend the analysis of Refs. 18 and 19 to the hyperbolic Penning and rf traps. The distribution function is a Maxwellian velocity distribu-

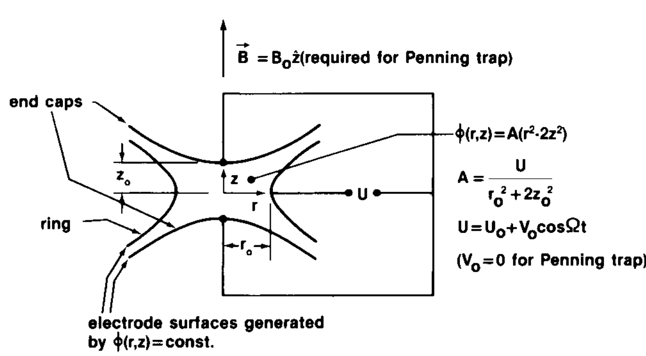

Fig. 2. Schematic representation of the electrode configuration for the Paul (rf) or Penning trap. Electrode surfaces are figures of revolution about the z axis and are equipotentials of $\phi(r, z) = A(r^2 - 2z^2)$ (cylindrical coordinates are used with the origin at the center of the trap). Typical dimensions are $\sqrt{2}z_0 = r_0 \cong 1$ cm. Typical operating parameters are the following: for the Paul trap, $V_0 = 300$ V, $\Omega/2\pi \cong 1$ MHz; for the Penning trap, $U_0 \cong 1$ V, $B \cong 1$ T.

tion superimposed upon a rigid rotation of frequency ω [positive (negative) values of ω denote rotation in the $+(-)$ θ direction]. For the Penning trap, this rotation is caused by the $\mathbf{E} \times \mathbf{B}$ drift and the pressure-gradient-induced drift [similar to $\mathbf{E} \times \mathbf{B}$ drift, where the term $(\partial n/\partial r)\hat{r}$ must be included with $E_r\hat{r}$].[20] In thermal equilibrium, these two effects in combination give rise to a rotation that is constant with radius. If the rotation is not rigid, then shear exists in the cloud; the resulting friction forces drive the cloud to thermal equilibrium. We emphasize that rigid rotation does not require a quadratic trap potential but only axial symmetry and thermal equilibrium. From the expression for the ion density, we arrive at Poisson's equation:

$$\frac{1}{r}\frac{\partial}{\partial r}\left(r\frac{\partial\phi}{\partial r}\right) + \frac{\partial^2\phi}{\partial z^2} = -4\pi q n_0 \times \exp\left\{-\left[q\phi - \tfrac{1}{2}m\omega\left(\frac{q}{|q|}\Omega_c + \omega\right)r^2\right]\Big/k_BT\right\} - 4\pi\rho', \quad (7)$$

where we must include the fictitious charge density, ρ', from the pseudopotential. In Ref. 19 it was shown that the general solution to Poisson's equation leads to axially symmetric ion densities that are constant out to a certain radius and then fall to zero in a universal way in a distance approximately equal to the Debye length, λ_D, given for a nonneutral plasma by

$$\lambda_D{}^2 = k_BT/4\pi n_0 q^2. \quad (8)$$

Although Ref. 19 specifically dealt with electrons in a Penning-type trap, Poisson's equation looks essentially the same for the rf trap, and therefore the general conclusion above is valid for both cases. (Recall that we are neglecting the micromotion.) Specific solutions are discussed in Ref. 19 for the Penning-type geometry and in Ref. 21 for the rf geometry.

As an example, for $T = 300$ K and $n_0 = 10^7/\text{cm}^3$, we have $\lambda_D \cong 0.38$ mm. At higher densities and lower temperatures, the general features of the density distribution noted above have been directly observed in Penning-type traps.[22,23] At higher temperatures and lower densities (where space charge becomes negligible and $\lambda_D \gtrsim$ ion-cloud dimensions) the density distributions become Gaussian; this has been directly observed in rf traps.[24,25]

Because of the laser-cooling experiments, it is interesting to consider the limiting case when $\lambda_D \ll$ cloud dimensions, i.e., when $T \rightarrow 0$. From the right-hand side of Eq. (6b), we can see that in the cloud interior, $q\phi - m(\Omega_c q/|q| + \omega)\omega r^2/2 \rightarrow 0$ in order for the density to be finite. Therefore, in the interior we have

$$\phi = \phi_I + \phi_T + \phi_{\text{ind}} = m\omega(\Omega_c q/|q| + \omega)r^2/2q. \quad (9)$$

The lack of z dependence in ϕ is to be expected since at low temperatures the outward z force from space charge would be expected just to cancel the restoring z force of the trap. In the case when the trap potential is quadratic [Eq. (2)], Eq. (9) can be written as

$$\phi_I = [m\omega(\Omega_c q/|q| + \omega)/2q - \alpha]r^2 - \beta z^2 - \phi_{\text{ind}} \quad (10\text{a})$$

$$= -\tfrac{2}{3}\pi q n_0(ar^2 + bz^2) - \phi_{\text{ind}}, \quad (10\text{b})$$

where Eq. (10b) is used to define a and b. From Poisson's equation, $2a + b = 3$. For a stable cloud of finite size, we must have $a, b > 0$; otherwise the ions are not confined. If the potential from the induced charges can be assumed constant over the ion cloud (this approximation is valid if the cloud's dimensions are small compared with r_0 and z_0), then ϕ_I is the potential distribution for a uniformly charged ellipsoid of revolution[23] of density n_0 whose spatial extent along the z axis we define as $2z_{\text{cl}}$ and whose diameter in the $z = 0$ plane we define as $2r_{\text{cl}}$. For simplicity we will therefore assume that ϕ_{ind} is constant over the ion cloud. If the dimensions and density of the ion cloud are large enough so that ϕ_{ind} is not constant over the ion cloud, then the cloud becomes elongated along z and expanded near the $z = 0$ plane.

For $a = b = 1$ the ion cloud is a sphere (i.e., $z_{\text{cl}} = r_{\text{cl}}$). For $a > 1 > b$ the cloud is a prolate ellipsoid ($z_{\text{cl}} > r_{\text{cl}}$), where[16,26]

$$a = k_p'\{1/[2(1 - k_p{}^2)] - \ln[(1 + k_p)/(1 - k_p)]/4k_p\}, \quad (11\text{a})$$

$$b = k_p'\{\ln[(1 + k_p)/(1 - k_p)]/2k_p - 1\}, \quad (11\text{b})$$

and where $k_p = [1 - (r_{\text{cl}}/z_{\text{cl}})^2]^{1/2}$ and $k_p' = 3(1 - k_p{}^2)/k_p{}^2$. For $a < 1 < b$ the cloud is an oblate ellipsoid ($r_{\text{cl}} > z_{\text{cl}}$), where

$$a = k_0'[\sin^{-1}(k_0)/2k_0 - (1 - k_0{}^2)^{1/2}/2], \quad (12\text{a})$$

$$b = k_0'[(1 - k_0{}^2)^{-1/2} - \sin^{-1}(k_0)/k_0], \quad (12\text{b})$$

and where $k_0 = [1 - (z_{\text{cl}}/r_{\text{cl}})^2]^{1/2}$ and $k_0' = 3(1 - k_0{}^2)^{1/2}/k_0{}^2$.

From Eq. (10a) and Poisson's equation, we can express n_0 as a function of ω and the trapping potentials:

$$n_0(\omega, \alpha, \beta) = \frac{m}{2\pi q^2}\left[-\omega(\Omega_c q/|q| + \omega) + \frac{q}{m}(2\alpha + \beta)\right]. \quad (13)$$

For the pure Penning trap, where $V_0 = 0$ and $2\alpha + \beta = 0$, we obtain the result of Ref. 23. The usual case for the rf trap is with $\Omega_c, \omega = 0$, and we obtain the result of Refs. 6 and 7. In practice, the minimum temperature and therefore the maximum density in an rf trap might be limited by rf heating,[24,27,28] where the condition $\lambda_D \ll r_{\text{cl}}, z_{\text{cl}}$ may not be obtained. If α and β are assumed fixed we find that the density is maximum when $\omega = -\Omega_c q/2|q|$:

$$n_0(\max) = \frac{m}{2\pi q^2}\left[\Omega_c{}^2/4 + \frac{q}{m}(2\alpha + \beta)\right]. \quad (14)$$

For the pure Penning trap ($2\alpha + \beta = 0$), we find[7,29] that $n_0(\max) = B_0{}^2/8\pi mc^2$. Also, the parameter a of Eq. (10b) is largest (i.e., $z_{\text{cl}}/r_{\text{cl}}$ is largest) for $\omega = -\Omega_c q/2|q|$. For the pure rf trap ($\Omega_c = 0$), this implies that $\omega = 0$ as expected, since spinning in either direction causes a centrifugal distortion that tends to make the ellipsoid more oblate. Equation (13) can be used to find ω if we assume that the cloud has a certain density n_0. We find that

$$\omega = -\Omega_c q/2|q| \pm [(\Omega_c/2)^2 + q(2\alpha + \beta - 2\pi q n_0)/m]^{1/2}. \quad (15)$$

In the pure Penning trap ($2\alpha + \beta = 0$), the solution for which $|\omega| < \Omega_c/2$ can be identified with the $\mathbf{E} \times \mathbf{B}$ drift magnetron motion and the solution for which $|\omega| > \Omega_c/2$ can be identified with the cyclotron frequency that is shifted by the radial electric field (see Section 6). For $n > n_0(\max)$ the ion orbits in the Penning trap are exponentially increasing.[7]

We note that Eq. (15) is not valid in the limit of a single ion, where one may want to substitute $n_0 \rightarrow 0$. Implicit in

Eq. (15) is the assumption that the axial force on an ion is zero. Equivalently, we assume that the cloud consists of many ions and that $\lambda_D \ll r_{cl}, z_{cl}$. In the limit of one ion in the trap, the axial force on an ion is due to the applied trapping fields (zero only at trap center). In addition, the requirement that $a > 0$ for clouds of finite size restricts the density n_0 to be greater than a minimum density given by $n_0(\min) = \beta/2\pi q$. At this minimum density, $a = 0$, and the cloud has infinite extent in the $z = 0$ plane. The requirement that $a > 0$ also restricts ω to values ranging from $\omega = -q\Omega_c/2|q| - [(\Omega_c/2)^2 + 2q\alpha/m]^{1/2}$ to $\omega = -q\Omega_c/2|q| + [(\Omega_c/2)^2 + 2q\alpha/m]^{1/2}$.

Finally, we can evaluate L_z for an ellipsoidal cloud of ions to find

$$L_z = n_0 \int_V \left[m r^2 \omega + r \frac{q}{c} A_\theta(r) \right] d^3\mathbf{x}$$

$$= \frac{2}{5} N m (\Omega_c q/2|q| + \omega) r_{cl}^2, \tag{16}$$

where $\int_V d^3\mathbf{x} = 4\pi r_{cl}^2 z_{cl}/3$ is the cloud volume.

A convenient dividing line between rf and Penning traps would seem to be when the radial electric force is absent, i.e., $\alpha = 0$. Therefore, in what follows, we will define the rf-trap mode as the case when the radial force that is due to the electric trapping fields is inward ($q\alpha > 0$) and the Penning-trap mode as the case when the radial force that is due to the electric trapping fields is outward ($q\alpha < 0$).

3. LASER SCATTERING

The problem that we wish to investigate is whether it is possible to observe angular-momentum changes induced by laser scattering in an ion cloud. For brevity, we will consider only a laser-beam/ion-cloud geometry in which these effects might be fairly strong; other interaction geometries could be similarly treated.

Consider the case of Fig. 3. We will assume that the spatial width of the laser beam is small compared with r_{cl} and z_{cl} and small enough that we can neglect the variation in first-order Doppler shift across the beam that is due to the cloud rotation. If the cloud is in thermal equilibrium, then ω is constant over the cloud; therefore the average y velocity of ions within the laser beam is $v_y = \omega r \cos\theta = \omega d$. For simplicity, we will assume that $|\omega| \ll \gamma$, where γ is the natural linewidth of the atomic transition to which the laser is nominally tuned. In this limit, photon scattering may be assumed to occur at an instant of time, and the momentum imparted to an ion is given by $\Delta\mathbf{p} = \hbar(\mathbf{k} - \mathbf{k}_s)$, where $\mathbf{k}$ and $\mathbf{k}_s$ are the photon wave vectors of the incident and scattered photons ($|\mathbf{k}| = |\mathbf{k}_s| = 2\pi/\lambda$).[4,5] Therefore the average torque from laser scattering is given by

$$T_L = \left\langle \frac{dL_z}{dt} \right\rangle_L = \int \frac{I(\mathbf{x})}{h\nu} \sigma(\mathbf{k} \cdot \mathbf{v}, T) \frac{h}{\lambda} dn(\mathbf{x}) d^3\mathbf{x}, \tag{17a}$$

where $I(\mathbf{x})$ is the intensity (power per unit area) of the laser beam, σ is the photon-scattering cross section, and $n(\mathbf{x})$ is the ion density. In the derivation of Eq. (17a), we have averaged over all angles of the reemitted photon. In general, the angular distribution of reemitted photons will not be isotropic [e.g., see Eqs. (8a) and (8b) of Ref. 5], but the torque that is due to photon reemission when averaged over angles will be zero, neglecting small relativistic corrections.[4] In the limit that the laser-beam dimensions are small compared with r_{cl}, z_{cl}, and d, and the density is nearly constant over the cloud ($\lambda_D \ll z_{cl}, r_{cl}$), then Eq. (17a) becomes

$$T_L = \left\langle \frac{dL_z}{dt} \right\rangle_L = \hbar 4\pi \dot{N}_L n_0 \sigma(v_y, T) d(r_{cl}^2 - d^2)^{1/2}/\lambda, \tag{17b}$$

where $\dot{N}_L$ is the number of incident laser photons per second and we note that σ has a line shape given in general by a Voigt profile[30] that is first-order Doppler shifted by a frequency $\omega d/\lambda$. As we noted earlier, if there is no damping, $|\langle L_z\rangle|$ will eventually increase. In principle the parameter a [Eq. (10b)] goes to zero; of course the edge of the cloud would touch the ring electrode before this condition is reached.

In practice, damping of $\langle L_z\rangle$ must be considered; it appears that this should come primarily from two sources: background neutral gas and imperfections in the trap electrodes that destroy axial symmetry and therefore prevent $\langle L_z\rangle$ conservation. Motional radiation damping should also be considered for electrons,[13,27,31] but this is expected to be a much weaker effect for ions. (In any case it would mimic background-gas damping.) Background-gas damping should occur in a similar way for the rf and Penning traps. However, since changes in L_z owing to trap asymmetries are expected to be qualitatively different for the two traps, they are treated separately.

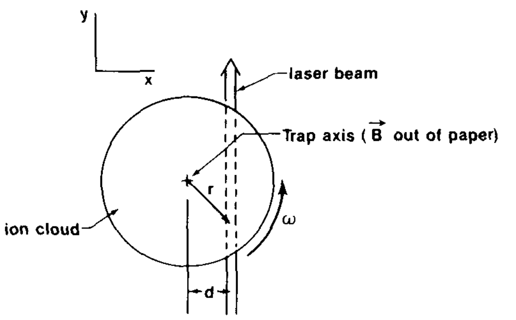

Fig. 3. Laser-beam–ion-cloud interaction geometry. The laser beam is assumed to be in the $z = 0$ plane; the radius of the ion cloud is r_{cl}. For the rf trap, laser scattering will tend to cause the cloud to spin in the direction shown. For the Penning trap, the direction of rotation shown ($\omega > 0$) is appropriate for negative ions; for positive ions the rotation is reversed ($\omega < 0$).

4. BACKGROUND-GAS DAMPING

An estimate of background-gas damping can be derived from measurements of ion mobility. The mobility K is defined[32] from the expression $v_d = KE$, where E is the electric field impressed on the ions in a drift experiment and v_d is the average drift velocity of the ions through some background gas. The drifting ions impart momentum to the gas at a rate

$$\frac{dp}{dt} = F = qE = qv_d/K. \tag{18}$$

Therefore, for the case of trapped ions, the torque that damps ion rotation is

$$\langle T_{bkg}\rangle = N\langle r dp/dt\rangle = -Nq\langle r^2\omega\rangle/K = -N\frac{2}{5}\frac{q}{K} r_{cl}^2\omega, \tag{19}$$

where the last equality is valid in the low-temperature limit, $\lambda_D \ll r_{cl}, z_{cl}$.

5. rf TRAP ($q\alpha > 0$)

We can get an idea of the magnitude of the change of L_z that is due to trap asymmetries by assuming that the pseudopotential has the form

$$\phi_T(r, z) = \alpha r^2 + \beta z^2 + \epsilon(x^2 - y^2). \qquad (20)$$

Assuming $\mathbf{B} = 0$, a single ion in this trap has the characteristic motions

$$x = x_1 \cos(\omega_x t + \theta_x),$$
$$y = y_1 \cos(\omega_y t + \theta_y), \qquad z = z_1 \cos(\omega_z t + \theta_z), \qquad (21a)$$

where the frequencies ω_x, ω_y, and ω_z are given by

$$\omega_x^2 = 2q(\alpha + \epsilon)/m, \qquad \omega_y^2 = 2q(\alpha - \epsilon)/m, \qquad \omega_z^2 = 2q\beta/m. \qquad (21b)$$

For $|\epsilon| \ll |\alpha|$, an ion initially in a nearly circular orbit defined by $x = \zeta \sin \omega_x t$, $y = \zeta \cos \omega_y t$ will find itself in a circular orbit of opposite sense after a time $\pi/|\omega_x - \omega_y|$. Hence, in this case, we estimate

$$T_\epsilon = \left\langle \frac{dL_z}{dt} \right\rangle_\epsilon \cong -L_z/\tau, \qquad \tau = \pi/2|\omega_x - \omega_y|. \qquad (22)$$

For a cloud of ions we could expect approximately the same dephasing time if space charge could be neglected, i.e., the ions behave independently. For a "cold" cloud, where the trapping force is essentially canceled by space charge, the situation is quite different. If we neglect ion–ion collisions, then ions drift through the cloud (which is now ellipsoidal in the x–y plane) and reflect from the edge of the ion-charge distribution. However, as an estimate we will still assume the validity of Eq. (22), where ω_x and ω_y are given by the free-space values of Eqs. (21).

To determine if spinning of the cloud induced by a laser beam could be observed, we have experimentally investigated a cloud of $^{198}Hg^+$ ions confined in a small rf trap.[33] In this experiment $r_0 = 455$ μm, $z_0 = 322$ μm, $\Omega/2\pi = 20$ MHz, $V_0 = 400$ V, and $U_0 = -12$ V. For a single ion in this approximately spherical well ($\alpha \cong \beta$) we would expect the secular frequency $\omega_z \cong \omega_x = \omega_y = (2q\alpha/m)^{1/2} = (2\pi)1.19$ MHz. For typical conditions, where $r_{cl} = 30$ μm, $d = 15$ μm, laser-beam waist size $\omega_0 = 15$ μm, and laser wavelength $\lambda = 194$ nm ($^2S_{1/2} \rightarrow {}^2P_{1/2}$ transition), we can ask under what conditions we would expect the cloud to spin at a frequency $\omega = (2\pi)0.5$ MHz. We choose this frequency because the corresponding first-order Doppler shift along the beam direction is about 250 MHz, which would be easily observable on the $^2S_{1/2} \rightarrow {}^2P_{1/2}$ transition. If we assume that $\lambda_D \ll r_{cl}, z_{cl}$, then we can use Eq. (13) to obtain $n_0 \cong 1.68 \times 10^{10}/\text{cm}^3$. The ions are observed[33] to be near room temperature (through the Doppler width on the $^2S_{1/2} \rightarrow {}^2P_{1/2}$ transition); hence we calculate that $\lambda_D = 9.2$ μm, and thus Eq. (13) should give a reasonable estimate of the density. From Eqs. (10) and (12) we then find that $z_{cl} \cong 25.8$ μm. In Eq. (17b) we write $\dot{N}_L\sigma = \dot{N}_s \pi \omega_0^2$, where $\dot{N}_s = \dot{N}_L\sigma/\pi\omega_0^2$ is the scatter rate per ion (for ions in the laser beam). We can then combine Eqs. (17b), (19), and (22) to obtain in steady state

$$\left\langle \frac{dL_z}{dt} \right\rangle_{\text{Total}} = \langle T_L + T_{\text{bkg}} + T_\epsilon \rangle = 0. \qquad (23)$$

For our specific example ($\omega/2\pi = 0.5$ MHz) we find that

$$\hbar[\dot{N}_s \times 3.0 \times 10^5 - n(\text{He}) \times 5.3 \times 10^{-2} - \Delta\nu_{xy} \times 2.3 \times 10^{10}] = 0, \qquad (24)$$

where we have assumed that the background gas is helium of density $n(\text{He})$ ($K = 19.6$ cm^2 V^{-1} sec^{-1} at standard pressure[34]) and we define $\Delta\nu_{xy} = |\omega_x - \omega_y|/2\pi$. If we first assume that the pressure of helium gas is small and $\Delta\nu_{xy} \cong 1$ kHz, we require that $\dot{N}_s \cong 7.7 \times 10^7$/sec (close to saturation) in order to spin the cloud at $\omega/2\pi = 0.5$ MHz. For the more typical scatter rates in this experiment, $\dot{N}_s \lesssim 10^6$/sec, we require that $\Delta\nu_{xy} \lesssim 13$ Hz in order to see the same ω. This would require a very small trap asymmetry in order for the effect to be seen, and in fact no spinning above $|\omega| = (2\pi)50$ kHz was observed, implying that $\Delta\nu_{xy} \gtrsim 130$ Hz for $\dot{N}_s = 10^6$/sec. Note that if $\Delta\nu_{xy} = 0$ and $p(\text{He}) = 6.65 \times 10^{-3}$ Pa (5×10^{-5} Torr), we need $\dot{N}_s \cong 3.1 \times 10^5$ to obtain $|\omega| = (2\pi)0.5$ MHz. Since $\dot{N}_s \gtrsim 3 \times 10^5$/sec and the helium pressure was less than 6.7×10^{-3} Pa in these experiments, we could determine that the lack of spinning was not due to background-gas damping.

We might expect to see a smaller dephasing (i.e., $\Delta\nu_{xy}$ smaller) for traps with weaker pseudopotential wells (ω_x, ω_y smaller), but it would still be necessary to maintain the high scatter rates (more difficult now because of the reduced densities). Of course one might become sensitive to smaller values of ω by probing narrower-linewidth transitions. In the low-temperature limit where the ion cloud becomes strongly coupled,[23,35] the dephasing effects might also be expected to be smaller if conditions of laminar flow or convection exist. Addition of an axial magnetic field may also help to prevent dephasing of L_z (see Appendix A). Finally, we remark that by adjusting U_0/V_0 it is possible to make the pseudopotential of Eq. (20) axially symmetric about either the x or the y axis, and therefore it should be possible to observe spinning about either axis experimentally. This possiblity was investigated in the Hg^+ experiment above, but $\dot{N}_s$ was not large enough and U_0/V_0 was not sufficiently stable for such spinning to be observed.

Therefore it should be possible (but perhaps difficult) to observe spinning in a rf trap. It is clearly a situation that is easily avoided. It has already been noted[4,36] that it is desirable in laser-cooling experiments to avoid axial symmetry in order to avoid recoil heating of the ions in a direction perpendicular to the laser beam.

6. PENNING TRAP ($q\alpha < 0$)

Angular momentum imparted to the cloud by light may be difficult to observe in an rf trap, however. In Penning traps it plays an important role. Since the radial electric trapping force and that which is due to space charge are outward, the only way to provide trapping is from a radial inward Lorentz force that is due to a rotation of the cloud as a whole. Therefore, even in the absence of a torque applied by the laser, the cloud must rotate at a frequency ω. It is easy to see that for the Lorentz force to be inward, ω must be negative for q positive and ω must be positive for q negative. From Eq. (16), we see that for the usual case, where $|\omega| < \Omega_c/2$, the total angular momentum is in the opposite sense to the mechanical angular momentum; that is, it is mostly angular momentum from the field [$\mathbf{x} \times \mathbf{A}$ term of Eqs. (1) or the term including Ω_c in Eq. (16)].

The case for a single trapped ion in a Penning trap interacting with a laser beam has been treated in some detail in Ref. 5. From the equation of motion

$$m\dot{\mathbf{v}} = -q\vec{\nabla}\phi + q(\mathbf{v} \times \mathbf{B})/c, \tag{25}$$

we determine that the motion in the z direction is harmonic with frequency $\omega_z = (2\beta q/\mathrm{m})^{1/2}$, and the motion in the x–y plane can be written in complex form:

$$x + iy = r_1 \exp(i\omega_1 t) + r_2 \exp(i\omega_2 t), \tag{26}$$

where $\omega_{1,2} = -\Omega_c q/2|q| \pm [(\Omega_c/2)^2 + 2q\alpha/\mathrm{m}]^{1/2}$ and where r_1 and r_2 are complex. The solutions for ω_1 and ω_2 are different from Eq. (15) for the reasons noted in Section 2. Note that these solutions are valid independently of the value of Ω_c or α and thus apply for either the Penning or the rf trap (see Appendix A).

From Eq. (26), it appears that the ω_1 and ω_2 components occur in an equal way. However, making the redefinitions[5]

$$x + iy = r_m \exp(i\omega_m t) + r_c \exp(i\omega'_c t), \tag{27}$$

$$\omega_m = -\frac{q}{|q|}\{\Omega_c/2 - [(\Omega_c/2)^2 + 2q\alpha/m]^{1/2}\}, \tag{28}$$

$$\omega_c' = -\frac{q}{|q|}\{\Omega_c/2 + [(\Omega_c/2)^2 + 2q\alpha/m]^{1/2}\}, \tag{29}$$

we can make the following observations: In the limit $\alpha \rightarrow 0$ we see that $\omega_m \rightarrow 0$ and $\omega_c' \rightarrow -q\Omega_c/|q|$; therefore the x–y motion is pure cyclotron motion. We identify the first term in Eq. (27) as the $\mathbf{E} \times \mathbf{B}$ drift magnetron motion of the guiding center of the cyclotron motion. The cyclotron frequency, ω_c', is now shifted by the radial electric fields. From the expression for the total energy in the x–y plane[5]

$$E_{xy}(\mathrm{total}) = m(q\Omega_c/2|q| + \omega_m)(\omega_m r_m^2 - \omega_c' r_c^2), \tag{30}$$

we see that the energy in the ω_c' motion is positive while that in the ω_m motion is negative (because it is mostly potential energy, $q\alpha r^2 < 0$).

As is shown in Ref. 5, momentum transfer or damping in the direction opposite the $\omega_m(\omega_c')$ motion causes r_m (r_c) to increase (decrease). As a consequence, to decrease both r_m and r_c, as is usually desired in laser-cooling experiments, we must cause momentum transfer simultaneously against the cyclotron motion and in the same direction as the magnetron motion.[5] Equivalently, we must reduce the cyclotron energy (this is similar to laser cooling of harmonically bound particles[5]) and *increase* the magnetron energy. For negative ions this can be accomplished by the laser-beam configuration shown in Fig. 3. The laser frequency ν_L should be tuned slightly below the rest frequency ν_0 ($\nu_0 = c/\lambda$), which has been first-order Doppler shifted by the magnetron rotation, i.e., $\nu_L \lesssim \nu_0(1 + |\omega| d/c)$. From the above considerations we also see why ion confinement in a Penning trap is normally a situation of unstable equilibrium. If any damping is present, then r_m increases until the ions strike the ring electrode. From similar considerations, the cyclotron motion should be damped by background-gas collisions.

We also note a qualitative difference between the Penning and the rf traps. For the Penning trap, by using the technique of laser cooling, it is experimentally possible[23] to achieve an amplitude for the cyclotron motion, r_c, much smaller than the amplitude of the magnetron motion, r_m. In this low-temperature limit the ion motion in the x–y plane is nearly circular, and L_z is conserved. If the trap potential is the distorted one given by Eq. (20), the solution for the x–y equations of motion is not a superposition of two circular motions as in Eq. (27) but a superposition of two elliptical motions (see Appendix A). Of course, in the limit that the asymmetry parameter ϵ goes to zero, these two elliptical solutions turn into the circular cyclotron and magnetron solutions of Eq. (27). In the low-temperature limit, the ion motion is elliptical (distorted magnetron motion), but fluctuations in L_z are small [expression (A10)]. This is to be contrasted with the rf trap, in which a distortion of the type in Eq. (20) causes a qualitatively different behavior for the motion and L_z can change significantly after a time τ [Eq. (22)].

The above considerations should apply when there is a cloud of ions except that $|\omega_m|$ [i.e., $|\omega| < \Omega_c/2$ in Eq. (15)] is shifted to higher values by space charge and $|\omega_c'|$ [i.e., $|\omega| > \Omega_c/2$ in Eq. (15)] is shifted to lower values. If we assume perfect axial symmetry and no damping, then it is interesting to consider the situation of Fig. 3 (appropriate for negative ions). First, if the laser beam is directed on the side of the trap axis opposite that shown, then a drag is applied to the magnetron motion that can increase the magnetron radius to large values or even expel the ions from the trap. This effect has been experimentally observed for Mg^+ (Ref. 37) and Be^+ ions. Now suppose the laser beam is directed as shown in Fig. 3. Further assume that the cyclotron motion is laser cooled ($T \rightarrow 0$) and that the cloud as a whole rotates at a frequency $|\omega_m| = |\omega| < \Omega_c/2$. As we continue to add angular momentum from the laser scattering, then we expect $|\omega|$ and the density n_0 to increase while the cloud radius, r_{cl}, decreases. This happens until $|\omega| = \Omega_c/2$ (i.e., $|\omega_m| = |\omega_c'| = \Omega_c/2$), at which point the maximum density is reached [Eq. (14)]. As more angular momentum is added by the laser, the rotation frequency $|\omega|$ becomes larger than $\Omega_c/2$ (i.e., $|\omega| = |\omega_c'|$ is now the cloud rotation frequency) and the density starts to decrease again and the cloud radius expands. In principle this continues to happen until the cloud radius reaches the ring electrode and ions are lost.

So far, the only experiment in which such effects were quantitatively studied is the one on $^9Be^+$.[23] In this experiment, small clouds of $^9Be^+$ ions were cooled and compressed, but the densities were limited to a value ($2 \times 10^7/\mathrm{cm}^3$) that was about an order of magnitude less than the maximum density given by Eq. (14). For these densities, the mean spacing between ions, $n^{-1/3}$, was about 37 μm while at the cyclotron temperatures achieved (T_c = 10–50 mK), $r_c \cong 1$ μm. We can first ask if the experimental limit was due to background-gas damping. For steady state, Eq. (23) must still apply (assuming here that $T_\epsilon = 0$). For the particular ion cloud of the first row in Table 1 of Ref. 23, we had $\omega_0 = 60$

μm, $\lambda = 313$ nm, $r_{cl} = 160\ \mu$m, $z_{cl} = 60\ \mu$m, $d \cong 50\ \mu$m, $n_0 = 2.1 \times 10^7/\text{cm}^3$, $T_z = 144$ mK, $N \cong 142$, and $\omega_m = (2\pi)37.3$ kHz. [For a single ion in the trap, $\omega_m = (2\pi)20.5$ kHz.] From Eq. (17b), we calculate that $|T_L| = \hbar \dot{N}_s \times 7.3 \times 10^4$. From Fig. 6 of Ref. 34, we take $K_0(\text{Be}^+, \text{He}) = 25\ \text{cm}^2\ \text{V}^{-1}\ \text{sec}^{-1}$; therefore, Eq. (19) gives $|T_{\text{bkg}}| = \hbar n(\text{He}) \times 7.7 \times 10^{-3}$. From the experiment we could estimate that $\dot{N}_s = 10^6$/sec. It was very unlikely that n(He) was larger than $10^8/\text{cm}^3$ based on heating data after the laser was turned off.[38] Therefore the limit on density was not due to background-gas damping.

It seems likely that the density was limited by imperfections in the trapping fields, which might lead to angular momentum's being coupled into the system.[38,39] Experimentally this density-limiting effect appeared very nonlinear in that the densities obtained were limited at a value that was fairly independent of laser power. (In the work reported in Ref. 23, varying the laser power by a factor of 10 had no measurable effect on the ion density.) Moreover, with the laser off the ions would rapidly heat at first[38] (~20 K/sec during the first 0.1 sec), but this heating would slow down (~1 K/sec from 10 to 20 sec), and the ions would remain in the trap for many hours. A possible mechanism for the density limit and the nonlinearity of the heating can be explained by assuming that the trap-symmetry axis is slightly tilted about the x axis by an angle δ with respect to the magnetic field. If we assume that the z axis is along the magnetic field, then the potential [assuming that $V_0 = 0$ in Eqs. (3)] is

$$\phi = \frac{U_0}{\xi^2}\,[2z^2 - r^2 + 3(y^2 - z^2)\sin^2\delta - 3zy\sin 2\delta]. \quad (31)$$

From this expression and the corresponding equations of motion, coupling between the z and y motions is clear. The frequencies of motion can be found from the eigenvalue problem (Ref. 40 and Appendix A), and one can also solve for the eigenvectors. Here we only point out that if the tilting is considered a perturbation, then there is an oscillating electric field in the y direction owing to the z motion

$$E_y = -\frac{\partial\phi}{\partial y} = 3zU_0\sin 2\delta/\xi^2 \quad (32)$$

that can drive the x–y motion. For a single particle in a Penning trap, and $\delta \ll 1$, this driving term at frequency $\cong \omega_z$ is nonresonant with ω_m and ω_c'; therefore no energy transfer between modes will occur. However, in a cloud of ions, the ω_m and ω_c' resonances are broadened by ion–ion collisions. Moreover, as n_0 increases because of compression, ω_m increases as noted above. In addition, the ion axial frequency ω_z' (for $T \neq 0$) is reduced by space charge from the free-space value. In the $^9\text{Be}^+$ experiment discussed above,[23] an estimate of ω_z' for $T \neq 0$ can be obtained by assuming that $\omega_z'/2\pi = v_z/4z_{cl}$, where $mv_z^2/2 = k_BT_z/2$. That is, we assume that the ion drifts across the ellipsoidal cloud (in the z direction) at its thermal velocity and reflects from the edge ($z \cong z_{cl}$). Clearly this is only a crude approximation since ion–ion collisions and collective effects will play a more important role.[14,15] However, using this model, we estimate that $\omega_z'/\omega_m \cong 1.3$, and therefore we have near-resonant coupling between the axial motion and the magnetron rotation. At lower densities and higher temperatures, ω_z'/ω_m becomes larger and resonance is avoided. The apparent resonant condition causes r_m to increase rapidly, which results in an increase in the ion cloud radius. Because of the resonant nature of this expansion, the process is called resonant particle transport.[14,39] A rapid increase in the cloud radius can cause rapid heating from the decrease in electrostatic energy as the cloud expands. This may account for the rapid heating observed immediately after the laser was turned off.[38] Thus it appears that distortions in trap symmetry may also be important for the Penning traps, particularly when high densities and low temperatures are desired. For the problem discussed here, the existence of such distortions may explain why we are unable to continue adding angular momentum to the ion cloud by laser scattering.

7. NEUTRAL-PARTICLE TRAPS

The same general considerations should apply to neutral-particle traps; the problem seems qualitatively simpler in that $q = 0$. Because of the short range of interparticle collisions, the situation for axially symmetric neutral traps should be similar to the case of ions in a rf trap in the low-density limit discussed above. Dephasing of angular momentum would be expected to be similar to that described in Section 5. Hence, as noted there, a small degree of trap asymmetry is probably required in order for spinning of the trapped sample to be observed.

8. CONCLUSIONS

In this paper we have been concerned primarily with angular momentum imparted to trapped particles by light scattering. As we noted earlier, this angular momentum could come from other sources, such as background gas, trap asymmetries, particle beams,[12] positive or negative feedback on charged-particle motions[12,13] (including radiative damping), and angular-momentum transfer from plasma waves.[14,15] Such considerations may modify the results of certain experiments such as those on electron– (or ion–) atom collisions.[41–43] For the case of ions in a Penning trap, it should be possible to compress the ion cloud at the center of the trap with a neutral-particle beam, although the cyclotron and axial degrees of freedom will be heated.

Therefore, in atomic-particle traps, one must in general take into account the angular momentum of the particles about a particular axis. If the trap has symmetry about this axis then these angular-momentum considerations are important in both the rf and the Penning ion traps and in neutral traps. We emphasize that it is the axial symmetry of the trap that is important for these angular-momentum considerations, not the adherence to the quadratic electric potentials that have been assumed, for simplicity, throughout this paper. If this axial symmetry is violated then it may in fact be difficult to observe angular-momentum effects in the rf or neutral traps. In Penning traps, such deviations from trap axial symmetry owing to electric-field distortions are not so important; in fact, angular-momentum effects, including the angular momentum imparted by laser scattering, play an important role in these experiments.

APPENDIX A

In Sections 5 and 6 we noted that if the electric potential is not axially symmetric, there is a significant difference in the behavior of L_z for the pure rf trap ($\mathbf{B} = 0$) and the Penning trap. To see how this difference might arise, we first examine the x–y motion when the trap potential is given by Eq. (20) and β and α are arbitrary. The equations of motion for a single ion are

$$\ddot{x} + 2q(\alpha + \epsilon)x/m = q\Omega_c\dot{y}/|q|, \tag{A1}$$

$$\ddot{y} + 2q(\alpha - \epsilon)y/m = -q\Omega_c\dot{x}/|q|. \tag{A2}$$

If we assume a solution $x = \mathrm{Re}[x_0 \exp(-i\omega t)]$, $y = \mathrm{Re}[y_0 \exp(-i\omega t)]$, we can write Eqs. (A1) and (A2) in matrix form:

$$M(\omega)\begin{bmatrix} x_0 \\ y_0 \end{bmatrix} = 0, \tag{A3}$$

where

$$M(\omega) = \begin{bmatrix} -\omega^2 + 2q(\alpha + \epsilon)/m & i\omega q\Omega_c/|q| \\ -i\omega q\Omega_c/|q| & -\omega^2 + 2q(\alpha - \epsilon)/m \end{bmatrix}. \tag{A4}$$

The normal mode frequencies are obtained from $\det M(\omega) = 0$, which has four roots, $\pm\,\omega_+$ and $\pm\omega_-$, where

$$2(\omega_\pm)^2 = \Omega_c^2 + 4q\alpha/m \pm (\Omega_c^4 + 8q\alpha\Omega_c^2/m + 16q^2\epsilon^2/m^2)^{1/2} \tag{A5}$$

or

$$2(\omega_\pm)^2 = \Omega_c^2 + 2\omega_r^2 \pm (\Omega_c^4 + 4\omega_r^2\Omega_c^2 + 4\omega_\epsilon^4)^{1/2}, \tag{A6}$$

where we have made the redefinitions $\omega_r^2 = 2q\alpha/m$ and $\omega_\epsilon^2 = 2q\epsilon/m = (\omega_x^2 - \omega_y^2)/2$. From Eq. (A3), we can find the following relationships between components of the eigenvectors:

$$\left(\frac{y_0}{x_0}\right)_{\omega=\pm\omega_+} = \mp iU_+,$$

$$U_+ = q[\Omega_c^2 - 2\omega_\epsilon^2 + (\Omega_c^4 + 4\omega_r^2\Omega_c^2 + 4\omega_\epsilon^4)^{1/2}]/2\omega_+\Omega_c|q|, \tag{A7}$$

and

$$\left(\frac{y_0}{x_0}\right)_{\omega=\pm\omega_-} = \mp iU_-,$$

$$U_- = q[\Omega_c^2 - 2\omega_\epsilon^2 - (\Omega_c^4 + 4\omega_r^2\Omega_c^2 + 4\omega_\epsilon^4)^{1/2}]/2\omega_-\Omega_c|q|. \tag{A8}$$

Therefore, the general solution is

$$x = r_+ \cos(\omega_+ t + \theta_+) + r_- \cos(\omega_- t + \theta_-),$$

$$y = -U_+ r_+ \sin(\omega_+ t + \theta_+) - U_- r_- \sin(\omega_- t + \theta_-). \tag{A9}$$

In the limit $\Omega_c \to 0$, these solutions are equivalent to those of Section 5 [Eqs. (21a) and (21b)] for the pure rf trap. If $\epsilon = 0$, then $|U_\pm| \to 1$, and we obtain the solutions of Section 6, where $|\omega_-| = |\omega_m|$ and $|\omega_+| = |\omega_c'|$. For $\epsilon \neq 0$, the solution [Eqs. (A9)] is a superposition of two elliptical motions at frequencies ω_+ and ω_-. For ϵ small, i.e., $\omega_\epsilon \ll \omega_r, \Omega_c$, we find that

$$\frac{q}{|q|}\,U_\pm \cong 1 - 2\omega_\epsilon^2/[\Omega_c^2 \pm (\Omega_c^4 + 4\Omega_c^2\omega_r^2)^{1/2}]. \tag{A10}$$

In general, L_z is a complicated function that can oscillate around zero. However, if we assume that only the (ω_+) or the (ω_-) mode is excited, then we obtain a simple expression:

$$L_{z\pm} = mr_\pm^2 \frac{q}{|q|}\frac{\Omega_c}{2}\,[\mp(1 + 4\omega_r^2/\Omega_c^2 + 4\omega_\epsilon^4/\Omega_c^4)^{1/2} + (U_\pm^2 - 1)\sin^2(\omega_\pm t + \theta_\pm) + 2\omega_\epsilon^2/\Omega_c^2]. \tag{A11}$$

If the ellipticity of the orbit is small, i.e., $||U_\pm| - 1| \ll 1$, then L_z has small fluctuations about a nonzero value. In the Penning trap, if we can assume the usual condition $|\omega_r/\Omega_c| \ll 1$, then we find that the magnetron orbit (ω_- solution) has $||U_-| - 1| \cong \omega_\epsilon^2/\omega_r^2$. In the rf trap, as $\Omega_c \to 0$, then $U_+ \to 0$ and $|U_-| \to \infty$; that is, the normal mode orbits are highly elliptical. However, if we assume that $\omega_r \gg \Omega_c \gg \omega_\epsilon$, then, from expression (A10), $||U_\pm| - 1| \cong \omega_\epsilon^2/\omega_r\Omega_c \cong |\omega_x - \omega_y|/\Omega_c$. Therefore, if we superimpose a magnetic field along the z axis so that $\Omega_c \gg |\omega_x - \omega_y|$, then the normal mode orbits would be nearly circular.

Based on the observations in Section 6 for the Penning trap, we might therefore make the following conjecture for a cloud of ions in either the Penning or the rf trap: If the x–y modes are nearly circular and if ω_+, ω_-, and the axial frequency (now shifted by space charge) are sufficiently different that mode coupling is suppressed, then the dephasing or damping of L_z might be small. Therefore in the rf trap we might expect to observe spinning more easily if we superimpose a magnetic field such that $\Omega_c \gg |\omega_x - \omega_y|$. For our $^{198}Hg^+$ example of Section 5, if $\Delta\nu_{xy} \cong 1$ kHz this would require that $B \gg 130$ G.

ACKNOWLEDGMENTS

We greatfully acknowledge the support of the U.S. Office of Naval Research and the U.S. Air Force Office of Scientific Research. We also thank J. C. Bergquist and L. R. Brewer for critical comments and helpful suggestions on the manuscript.

REFERENCES

1. A. Ashkin, "Applications of laser radiation pressure," Science **210,** 1081–1088 (1980).
2. W. D. Phillips, ed., *Laser-Cooled and Trapped Atoms*, Nat. Bur. Stand. (U.S.) Spec. Publ. **653,** (1983); Prog. Quantum Electron. **8,** 115–259 (1984).
3. D. J. Wineland, W. M. Itano, J. C. Bergquist, J. J. Bollinger, and J. D. Prestage, "Spectroscopy of stored atomic ions," in *Atomic Physics 9*, R. S. Van Dyck, Jr., and E. N. Fortson eds. (World Scientific, Singapore, 1985), pp. 3–27.
4. D. J. Wineland and W. M. Itano, "Laser cooling of atoms," Phys. Rev. A **20,** 1521–1540 (1979).
5. W. M. Itano and D. J. Wineland, "Laser cooling of ions stored in harmonic and Penning traps," Phys. Rev. A **25,** 35–54 (1982).
6. H. G. Dehmelt, "Radiofrequency spectroscopy of stored ions. I and II," Adv. At. Mol. Phys. **3,** 53–72 (1967); **5,** 109–154 (1969).
7. D. J. Wineland, W. M. Itano, and R. S. Van Dyck, Jr., "High resolution spectroscopy of stored ions," Adv. At. Mol. Phys. **19,** 135–186 (1983).
8. A quantum mechanical treatment of rf trapping is given in R. J. Cook, D. G. Shankland, and A. L. Wells, "Quantum theory of

Mechanical Effects of Light

particle motion in a rapidly oscillating field," Phys. Rev. A **31**, 564–567 (1985).

9. E. Fischer, "Die dreidimensionale Stabilisierung von Ladungsträgern in einem Vierpolfeld," Z. Phys. **156**, 1–26 (1959).
10. F. G. Major and H. G. Dehmelt, "Exchange-collision technique for the rf spectroscopy of stored ions," Phys. Rev. **170**, 91–107 (1968).
11. H. A. Schuessler, E. N. Fortson, and H. G. Dehmelt, "Hyperfine structure of the ground state of $^3He^+$ by the ion-storage exchange-collision technique," Phys. Rev. **187**, 5–38 (1969).
12. D. J. Wineland, R. E. Drullinger, J. C. Bergquist, and W. M. Itano, "Laser induced magnetron compression (expansion) of ions stored in a Penning trap," Bull. Am. Phys. Soc. **24**, 1185 (1979).
13. W. D. White, J. H. Malmberg, and C. F. Driscoll, "Resistive wall destabilization of diocotron waves," Phys. Rev. Lett. **49**, 1822–1826 (1982).
14. D. L. Eggleston, T. M. O'Neil, and J. H. Malmberg, "Collective enhancement of radial transport in a nonneutral plasma," Phys. Rev. Lett. **53**, 982–984 (1984).
15. J. D. Crawford, T. M. O'Neil, and J. H. Malmberg, "Effect of nonlinear collective processes on the confinement of a pure electron plasma," Phys. Rev. Lett. **54**, 697–700 (1985).
16. The potential for a uniformly charged ellipsoid of revolution can be found in W. D. MacMillan, *The Theory of the Potential* (Dover, New York, 1958), pp. 17 and 45; O. D. Kellog, *Foundation of Potential Theory* (Ungar, New York, 1929), p. 195.
17. L. D. Landau and E. M. Lifshitz, *Statistical Physics* (Addison-Wesley, Reading, Mass., 1974).
18. J. H. Malmberg and T. M. O'Neil, "Pure electron plasma, liquid, and crystal," Phys. Rev. Lett. **39**, 1333–1336 (1977).
19. S. A. Prasad and T. M. O'Neil, "Finite length thermal equilibria of a pure electron plasma column," Phys. Fluids **22**, 278–281 (1979).
20. T. M. O'Neil and C. F. Driscoll, "Transport to thermal equilibrium of a pure electron plasma," Phys. Fluids **22**, 266–277 (1979).
21. L. S. Cutler, R. P. Giffard, and M. D. McGuire, "Mercury-199 trapped ion frequency standard: recent theoretical progress and experimental results," in *Proceedings of the 37th Annual Symposium on Frequency Control*, 1983. (Copies available from Systematics General Corporation, Brinley Plaza, Rt. 38, Wall Township, N.J. 07719), pp. 32–36; "Thermalization of ^{199}Hg ion macromotion by a light background gas in an rf quadrupole trap," Appl. Phys. B **36**, 137–142 (1985).
22. J. S. deGrassie and J. H. Malmberg, "Waves and transport in the pure electron plasma," Phys. Fluids **23**, 63–81 (1980).
23. J. J. Bollinger and D. J. Wineland, "Strongly coupled nonneutral ion plasma," Phys. Rev. Lett. **53**, 348–351 (1984).
24. R. D. Knight and M. H. Prior, "Laser scanning measurements of the density distribution of confined $^6Li^+$ ions," J. Appl. Phys. **50**, 3044–3049 (1979).
25. H. Schaaf, V. Schmeling, and G. Werth, "Trapped ion density distribution in the presence of He-buffer gas," Appl. Phys. **25**, 249–251 (1981).
26. J. B. Jeffries, S. E. Barlow, and G. H. Dunn, "Theory of space-charge shift of ion cyclotron resonance frequencies," Int. J. Mass Spectrom. Ion Phys. **54**, 169–187 (1983).
27. D. A. Church and H. G. Dehmelt, "Radiative cooling of an electrodynamically contained proton gas," J. Appl. Phys. **40**, 3421–3424 (1969).
28. H. G. Dehmelt, "Stored ion spectroscopy," in *Advances in Laser Spectroscopy*, F. T. Arecchi, F. Strumia, and H. Walther, eds. (Plenum, New York, 1983), pp. 153–187.
29. D. J. Wineland, "Spectroscopy of stored ions," in *Precision Measurement and Fundamental Constants II*, B. N. Taylor and W. D. Phillips, eds., Natl. Bur. Stand. (U.S.) Spec. Publ. **617** (1984), p. 83–92.
30. J. T. Davies and J. M. Vaughan, "A new tabulation of the Voigt profile," Astrophys. J. **137**, 1302–1305 (1963).
31. H. G. Dehmelt and F. L. Walls, "Bolometric technique for the rf spectroscopy of stored ions," Phys. Rev. Lett. **21**, 127–131 (1968).
32. E. W. McDaniel, *Collision Phenomena in Ionized Gases* (Wiley, New York, 1964), pp. 426–482.
33. J. C. Bergquist, D. J. Wineland, W. M. Itano, H. Hemmati, H.-U. Daniel, and G. Leuchs, "Energy and radiative lifetime of the $5d^96s^2\ ^2D_{5/2}$ state in Hg II by Doppler-free two-photon laser spectroscopy," Phys. Rev. Lett. (to be published).
34. L. M. Chanin and M. A. Biondi, "Mobilities of mercury ions in helium, neon and argon," Phys. Rev. **107**, 1219–1221 (1957).
35. S. Ichimaru, "Strongly coupled plasmas: high density classical plasmas and degenerate electron liquids," Rev. Mod. Phys. **54**, 1017–1059 (1982).
36. W. Neuhauser, M. Hohenstatt, P. E. Toschek, and H. G. Dehmelt, "Localized visible Ba^+ mono-ion oscillator," Phys. Rev. A **22**, 1137–1140 (1980).
37. R. E. Drullinger, D. J. Wineland, and J. C. Bergquist, "High-resolution optical spectra of laser cooled ions," Appl. Phys. **22**, 365–368 (1980).
38. J. J. Bollinger, J. D. Prestage, W. M. Itano, and D. J. Wineland, "Laser cooled atomic frequency standard," Phys. Rev. Lett. **54**, 1000–1003 (1985).
39. C. F. Driscoll and J. H. Malmberg, "Length dependent containment of a pure electron-plasma column," Phys. Rev. Lett. **50**, 167–170 (1983).
40. L. S. Brown and G. Gabrielse, "Precision spectroscopy of a charged particle in an imperfect Penning trap," Phys. Rev. A **25**, 2423–2425 (1982).
41. M. D. McGuire and E. N. Fortson, "Penning-trap technique for studying electron-atom collisions at low energy," Phys. Rev. Lett. **33**, 737–739 (1974).
42. G. Graff, F. G. Major, R. W. H. Roeder, and G. Werth, "Method for measuring the cyclotron and spin resonance of free electrons," Phys. Rev. Lett. **21**, 340–342 (1968).
43. G. Graff and M. Holzscheiter, "Method for trapped ion polarization and polarization detection," Phys. Lett. **79A**, 380–382 (1980).

(see overleaf)